PAPER

Applicability of d-excess and ^{17}O-excess as groundwater tracers for determination of recharge area

Isao Machida[1] · Masahiko Ono[1] · Takafumi Kamitani[2] · Yasuhide Muranaka[3]

Abstract

Methods to determine the recharge elevation of groundwater using the altitude effect of δD and δ^{18}O have been extensively applied in hydrogeological investigations. The secondary parameter d-excess has also been used as a groundwater tracer. In this study, to examine the usefulness of these tracers along with ^{17}O-excess, ~160 groundwater samples were collected from a humid region at the foot of Mt. Fuji, Japan. The sampling area covered 40×45 km, with most sampling sites located below 1,000 m above sea level. The relatively low elevation and small scale of the basin allowed for examination of the elevation-dependence of groundwater isotopes. Using high-precision isotope analyses, a low lapse rate but clear elevation-dependence in spring waters was observed for d-excess (0.18‰·100 m^{-1}). The recharge elevation determined by d-excess correlated with those by δD and δ^{18}O, indicating that d-excess has high potential as a groundwater tracer for the determination of recharge elevation. On the other hand, ^{17}O-excess in groundwater held small spatial variation, with an average of 25 per meg in the horizontal direction and a lapse rate of 0.6 per meg·100 m^{-1}. The low lapse rate compared to the analysis error inhibits its usefulness as a tracer. The fact that the recharge elevation determined by δD, δ^{18}O, and d-excess were similar indicates that the combination of these tracers could increase the reliability of the results.

Keywords Stable isotopes · d-excess · ^{17}O-excess · Lapse rate · Japan

Introduction

Deuterium and oxygen-18 in water have been commonly employed as natural tracers to estimate the origin, age, history, and flow path of groundwater (Clark and Fritz 1997; Mazor 1997; Kendall and McDonnell 1998; Mook 2001; Yamanaka 2020). In particular, the isotope altitude effect (i.e., elevation effect), a phenomenon in which precipitation becomes isotopically lighter at higher elevations, has been useful for determining the groundwater recharge elevation

as summarized by Jasechko (2019). The altitude effect is produced by: (1) rain-out from vapor orographically lifted or Rayleigh distillation with different condensation temperatures with temperature lapse rate (≈ 0.6 °C · 100 m^{-1}), and (2) evaporation from raindrops (Friedman et al. 1962; Moser and Stichler 1974; Clark and Fritz 1997; Kendall and McDonell 1998; Gonfiantini et al. 2001; Mook 2001; Yamanaka 2020). This effect has been observed across many areas, ranging from -0.6 to -0.1‰ · 100 m^{-1} for δ^{18}O (Siegenthaler 1979; Yurtsever and Gat 1981; Mazor 1997; Machida 2000; Mook 2001; Yamanaka et al. 2016) and changes depending on the direction of the slope against the wind direction (e.g., Scholl et al. 1996; Machida 2005; Yasuhara et al. 2007).

On the other hand, one of the secondary parameters, d-excess, also has been used as a groundwater tracer in several areas (Cruz-Sun Julian et al. 1992; Paar et al. 2019). d-excess was defined by Dansgaard (1964) according to Eqs. (1) and (2):

$$\text{d-excess} = \delta D - 8\delta^{18}O \qquad (1)$$

✉ Isao Machida
i-machida@aist.go.jp

[1] Geological Survey of Japan, National Institute of Advanced Industrial Science and Technology, Chuo 7, 1-1-1 Higashi Tsukuba-shi, Ibaraki 305-8567, Japan

[2] Research and Development Management Division, Shizuoka Prefectural government, 9-6 Ote-machi, Aoi-ku, Shizuoka-shi, Shizuoka 420-8601, Japan

[3] Shizuoka Institute of Environment and Hygiene, 232-1 Yainaba, Fujieda-shi, Shizuoka 426-0083, Japan

$$\delta = \left(\frac{R_{\text{sample}}}{R_{\text{SMOW}}} - 1 \right) \times 1000 \qquad (2)$$

where R is the ratio of heavy to light isotopes: ($^{18}O/^{16}O$) for ^{18}O; ($^{2}H/^{1}H$) for deuterium; and the SMOW is the reference, standard mean ocean water (Craig 1961a). From this definition, the d-excess of the Global Meteoric Water Line (GMWL: $\delta D = 8\delta^{18}O + 10$, as defined in Craig 1961b) is the y-intercept (10), and reflects a kinetic isotopic fractionation process when water vapor is formed from the ocean, whereas the slope reflects the Rayleigh process when precipitation is formed from vapor. When the humidity is low ($\leq 50\%$), the vapor is strongly depleted of $\delta^{18}O$ compared to that of the ocean, and the produced precipitation contains high d-excess; however, at a humidity of ~85%, the precipitation plots are very close to the GMWL (Clark and Fritz 1997).

The d-excess also tends to increase with elevation, but the lapse rate is different by region, as well as δD and $\delta^{18}O$. A drastic change in d-excess with elevation was produced by the mixing of the local orographic cloud (for precipitation in Italy, ~$0.6‰ \cdot 100\ m^{-1}$, Liotta et al. 2006) and by the mixing of water derived from different seasons (for surface water in Tibetan Plateau, ~$2.2‰ \cdot 100\ m^{-1}$; Dong et al. 2018). Without such mixings, the evaporation of raindrops below the cloud base causes its elevation-dependence in arid and semiarid regions (Ehhalt et al. 1963; Gat 1971; Gat and Dansgaard 1972; Clark and Fritz 1997). Additionally, some researchers have reported that d-excess in the precipitation or river water change with elevation in more humid areas—for example, Cruz-San Julian et al. (1992) observed individual precipitation with a lapse rate of ~$0.5‰ \cdot 100\ m^{-1}$ in coastal areas in eastern Spain. Gonfiantini et al. (2001) observed a lapse rate of ~$0.1‰ \cdot 100\ m^{-1}$ for monthly precipitation observed in Cameroon and Bolivia, located in tropical regions, whereas Liebminger et al. (2006) compiled precipitation data for ~30 years across 12 stations in Austria with relative humidity (RH) of 87% and found elevation changes in d-excess (lapse rate of $0.36‰ \cdot 100\ m^{-1}$). Bershaw et al. (2012) showed a lapse rate of ~$0.3‰ \cdot 100\ m^{-1}$ using the data obtained by Garzione et al. (2000), who collected stream waters in tributaries of the Kali Gandhaki River, Himalaya. Wakiyama et al. (2013) revealed lapse rates ranging from 0.16 to $0.32‰ \cdot 100\ m^{-1}$ in precipitation in central Japan, while Bershaw et al. (2020) found a lapse rate of ~0.23–$0.24‰ \cdot 100\ m^{-1}$ along the moist, windward side (RH > 75%) of the stream waters from the Olympic Mountains, Oregon, United States. In particular, Gonfiantini et al. (2001) and Bershaw et al. (2012) emphasized that such change could be produced by rain-out, using the Rayleigh condensation model. The current consensus would be that the elevation dependence of d-excess is produced by two mechanisms, the rain-out and evaporation, and the lapse rates range from 0.1 to $0.5‰ \cdot 100\ m^{-1}$ in the humid regions

unless there is mixing with other sources. The contribution of the two mechanisms is still unknown, and may be important because the same phenomenon can occur in many areas on Earth. Although the lapse rate of d-excess is sometimes only $0.1‰ \cdot 100\ m^{-1}$, it may be a useful tracer to determine recharge elevation even in small-scale basins by using high-precision analyses.

Alternatively, the precision of $\delta^{17}O$ measurement has continued to improve (Steig et al. 2014), often represented by an index called ^{17}O-excess rather than the δ value itself (Barkan and Luz 2007). In the field of hydrogeology, the δ value is generally expressed by multiplying the right side by 1000 (as in Eq. 2); accordingly, ^{17}O-excess is expressed by:

$$^{17}O\text{-excess} \times 10^{-6} = \ln\left(10^{-3}\delta^{17}O + 1\right) - 0.528 \ln\left(10^{-3}\delta^{18}O + 1\right) \qquad (3)$$

Corresponding to the GMWL for the $\delta^{17}O$-$\delta^{18}O$ relationship, Luz and Barkan (2010) proposed the following straight line from 52 global water samples:

$$\ln\left(10^{-3}\delta^{17}O + 1\right) = 0.528 \ln\left(10^{-3}\delta^{18}O + 1\right) + \left(33 \times 10^{-6}\right) \qquad (4)$$

That is, natural waters maintain a linear relationship between $\ln(10^{-3}\delta^{17}O + 1)$ and $\ln(10^{-3}\delta^{18}O + 1)$, with a slope (0.528) resulting from the assumption that vapor condensation occurs in the Rayleigh process (Barkan and Luz 2007). The ^{17}O-excess throughout water circulation is assumed to be stable during the phase change under equilibrium, but it changes under a nonequilibrium evaporation process. The characteristics are similar to d-excess, where the latter is affected by both temperature and RH (even in equilibrium), but ^{17}O-excess is solely sensitive to RH during evaporation (Barkan and Luz 2007).

Hydrological studies using ^{17}O include analyses of Antarctic ice cores (Landais et al. 2008, 2012), assessing the relationship between ^{17}O-excess in oceanic water vapor and RH (Uemura et al. 2010), and an examination of the global distribution of ^{17}O-excess in natural waters (Luz and Barkan 2010). Recently, some researchers have also focused on the relationship between d-excess and ^{17}O-excess to examine the evaporation of water. Landais et al. (2010) analyzed precipitation samples in West Africa, revealing a relationship between d-excess and ^{17}O-excess with RH. The ratio of change in ^{17}O-excess:d-excess was ~1 per meg $\cdot ‰^{-1}$, and evaporation from raindrops was a key process for controlling the d-excess and ^{17}O-excess in precipitation. Li et al. (2015) demonstrated a national-scale map of ^{17}O-excess in precipitation over the US (using tap water as a proxy), finding that the ^{17}O-excess was highly latitude-dependent at the continental scale, and high correlation among ^{17}O-excess, d-excess, and average annual precipitation near the Gulf of Mexico, likely due to evaporation. Their observed change in ^{17}O-excess with respect to d-excess was ~4.0 per meg $\cdot ‰^{-1}$ near the Gulf of

Mexico. Tsuchihara et al. (2016) found a seasonal fluctuation of ^{17}O-excess in precipitation positively correlated to d-excess in Ibaraki Prefecture, Japan. Since it is common that the d-excess in precipitation decreased to ~5‰ in the summer and increased to ~30‰ in winter within the Japanese mainland (Tanoue et al. 2013; Ichiyanagi and Tanoue 2016), Tsuchihara et al. (2016) attributed it to seasonal changes of water vapor origins. In addition, there was a positive relationship between d-excess and ^{17}O-excess in the evaporated rice paddy water, with a ratio of change of 1.2 per meg · ‰$^{-1}$. The average value of ^{17}O-excess in the shallow groundwater ($n = 52$) was 26 per meg. That is, the relationship between d-excess and ^{17}O-excess in natural waters has been reported to range from 1 to 4 per meg · ‰$^{-1}$ by previous studies.

Although hydrological d-excess and ^{17}O-excess studies using high-precision analyses are underway, local-scale research remains insufficient; in particular, to the best of the authors' knowledge, no studies have discussed their groundwater spatial distributions for a basin with a scale of several 10s of kilometers in humid regions. In this study, these distributions were clarified, and their potential as groundwater tracers to determine the recharge elevation was examined. For this purpose, Mt. Fuji and its surroundings (Japan) were selected as the research area (Fig. 1), in part for its extensive historical use in hydrogeological research to aid in the interpretation of the data obtained from this study.

Materials and Methods

Research area

The total research area covers ~40×45 km^2, 100 km west–southwest of Tokyo in Japan (Fig. 1), and contains Mt. Fuji (peak elevation, 3,776 m). The area was subdivided into seven sections: N, E, H, SE, SW, W, and F (further details are provided in the next section). According to the seven weather stations located within the subsections, the average annual rainfall ranged from 915 to 2,845 mm for 1976–2020 (Table 1; Japan Meteorological Agency 2021), with the maximum recorded at Gotenba (E), and minimums at Lake Kawaguchi (N) and Mishima (H; 915 and 1,011 mm · y^{-1}, respectively). There are no precipitation data for the summit of Mt. Fuji as the winds are too strong for reliable measurements, although the heaviest rains occur during the rainy and typhoon seasons (June–September), where ~60–70% of the annual precipitation occurs within the summer. Humidity data were obtained at two stations with the least rainfall: Lake Kawaguchi (N) and Mishima (H) (average RH = 72%).

The research area further includes Mt. Ashitaka and Hakone distinct. The most recent eruption of Mt. Fuji occurred 300 years ago, whereby the mountain body was covered by permeable, volcanic ejecta. Due to surface geology, there are no ephemeral rivers except in the lower part of the mountain body. Mt. Ashitaka and Hakone began erupting ~0.40 and 0.65 Ma, respectively, with the former terminating its activity ~0.1 Ma, and the latter still presently experiencing minor eruptions (Yui and Fujii 1989; Nagai and Takahashi 2008). Accordingly, the geology of Mt. Fuji, Mt. Ashitaka, and Hakone is characterized by Quaternary volcanoes.

There are two particularly important studies discussing the spatial distributions of δD and δ^{18}O in natural waters across the research area, Nakai et al. (1995) and Yasuhara et al. (1997). The reproducibilities of the δD and δ^{18}O analyses were ±1.5 and ±0.1‰, respectively (Nakai et al. 1995), and for δD it was ±1.5‰, with no mention of δ^{18}O by Yasuhara et al. (1997). The Nakai et al. 1995 research project collected a total of 128 groundwater samples and found that the δ^{18}O ranged from −12.2 to −7.0‰. Light and heavy δ were obtained in the N and SE areas, respectively, and this phenomenon was attributed to the difference in elevation (i.e., the altitude effect, where the elevation of the N area is higher than all others; Fig. 1). They also noticed a negative linear correlation between δ^{18}O and d-excess in the well water of the SE area. Ultimately, they derived a slope of 5.6 for the δ^{18}O–δD relationship. Yasuhara et al. (1997, 2007) measured isotope components for 60 groundwater samples, which maintained a slope of 8, and an intercept of 13.5, with an estimated lapse rate of −2‰ · 100 m^{-1} for δD (Ono et al. 2018). Groundwater with light δ was found in the N area, which was attributed to the "rain shadow effect" (Scholl et al. 1996) caused when moist vapor coming from the windward side moves leeward of the mountain body, losing the water vapor under the Rayleigh process. From the estimated wind flow lines in the entire research area during heavy rainfall (Kizawa et al. 1969), two predominant movements of vapor flow are considered: water vapor brought from the south which moved mainly to area W, and partly to area E. The other vapor comes from the east, passing through the north of Hakone, bringing much precipitation to area E, and moving to area N. Accordingly, the light δ recorded in groundwater for the N area was due to higher elevation and water vapor movement.

All models of groundwater flow in area SW revealed "layers", where deep and shallow groundwater are recharged at high and low elevations, respectively (Nakai et al. 1995; Yasuhara et al. 1997, 2007; Ono et al. 2018). Horizontally, the groundwater recharged at Mt. Ashitaka and Mt. Fuji is distinguished by the NO$_3^-$ concentrations (Shikazono et al. 2014) and δ values (Ono et al. 2018). In addition, Ono et al. (2018) identified groundwater mixed with the inflow of the Fuji River, flowing west from Fuji City, by low vanadium concentration. Accordingly, the hydrogeology in the SW area has been well characterized and is a primary reason why the SW area was selected for focused discussion later.
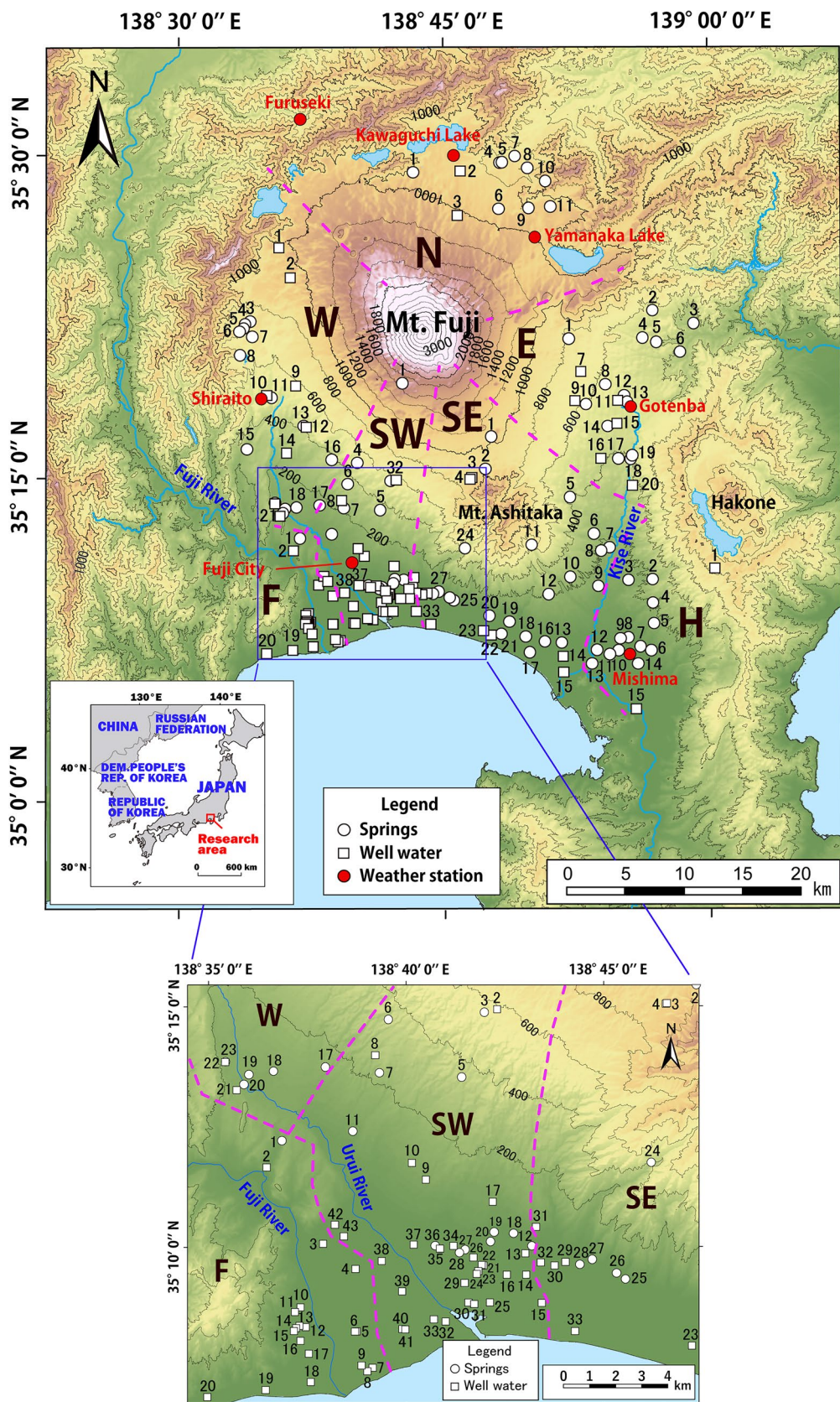
Fig. 1 Research area and sampling points near Mt. Fuji, Japan. The pink dotted lines indicate the boundaries of the areas: N, E, H, SE, SW, W, and F

Division of research area

Figure 1 shows the groundwater sampling points (spring and well). As mentioned earlier, the isotopic composition of precipitation in Mt. Fuji changed depending on slope and elevation. The research area was thus divided into seven areas: north (N), east (E), southeast (SE), southwest (SW), west (W), Hakone (H), and the Fuji River (F). The N–E, N–W, and E–SE boundaries are topographical divides. The SE and H areas are bordered by the Kise River. In area H, there were two types of groundwater: one is the groundwater flowing from Hakone (Ueno et al. 1998 and the other is Mishima Springs (including Nos. 10 and 11 in Fig. 1). Mishima Springs has an estimated total discharge of 1.7×10^6 m$^3 \cdot$ day^{-1} that passes through the Mishima Lava, and originating at an elevation of 1,700 m in the E area (Ochiai and Kawasaki 1970). Accordingly, the groundwater in the H area must be largely influenced by external regions. The SE–SW boundary is determined based on the differences in recharge area, where the groundwater can be clearly identified by the NO_3^- and δ values (see section 'Research area'). The groundwater on the SE side is presumed to be recharged on Mt. Ashitaka, and the SW side is recharged on Mt. Fuji. The SW–F boundary is a curved line reflecting the difference in their sources. Some groundwater in area F is mixed with the recharged water from the Fuji River (as identified by the low vanadium concentrations; Ono et al. 2018), whereas the other parts of area F are recharged in the western hills of the Fuji River. The W–SW boundary is based on the topography and water-table map shown by Ono et al. (2018).

Measurements

Groundwater samples were collected using 100-ml polyethylene bottles after filtering using a 0.45-μm filter and sealed tightly to prevent evaporation (Ono et al. 2016, 2018) and stored in a refrigerator. Ono et al. (2016) collected groundwater twice in different years and confirmed that there were no major annual changes in δD and δ^{18}O except in several well waters. A linear relation was observed between δD and δ^{18}O across the 2 years, maintaining a slope of 1.000 and 0.998, respectively, with intercepts of 0 and coefficients of determination (R^2) equal to 1.000; thus, the isotope compositions in the spring and most well waters of the research area did not show any annual changes, and can be regarded as representatives.

Oxygen and hydrogen stable isotopic compositions (δ^{17}O, δ^{18}O, and δD) were measured using a liquid water isotope analyzer (L2140-i, Picarro, USA) that employs a cavity ring-down spectrometer. VSMOW-2, GISP, and SLAP2 provided by the International Atomic Energy Agency (Martin and Gröning 2009; Wise and Watters 2012) were used as standard solutions, and all δ values in this study were normalized on the VSMOW-SLAP scale (Schoenemann et al. 2013). The precision of δ^{17}O and ^{17}O-excess analyses, including the long-term drift, were checked over multiple months via repeated measurements of the GISP, revealing an ^{17}O-excess of 22 ± 9 per meg, agreeing well with previously published data, and indicative of data reliability (Table 2).

Measurements of the isotopes were carried out during 2016–2017. A total of 12 measurements for each water

Table 1 Average values of precipitation, temperature, and relative humidity from 1976 to 2020 across seven weather stations in the research area (Japan Meteorological Agency, 2021)

Weather station	Area	Longitude (°)	Latitude (°)	Elevation (m)	Precipitation (mm/year)	Temperature (°C)	Relative humidity (%)
Lake Kawaguchi	N	138.760	35.500	860	915	10.7	73.4
Lake Yamanaka	N	138.837	35.437	992	2,277	9.2	–
Gotenba	E	138.927	35.305	472	2,845	12.9	–
Mishima	H	138.925	35.113	21	1,011	16.0	71.4
Fuji City	SW	138.663	35.185	66	2,140	15.9	–
Shiraito	W	138.578	35.312	530	2,286	–	–
Furuseki	N, W	138.615	35.528	552	1,659	12.2	–

Table 2 Isotopic analyses of IAEA standard solution, GISP

Source	δD ‰ ± 1σ	δ^{17}O (‰)	δ^{18}O (‰)	d-excess (‰)	^{17}O-excess per meg ± 1σ
Wise and Watters (2012)	-189.5 ± 0.1	–	-24.78 ± 0.01	–	–
Schoenemann et al. (2013)	–	-13.16 ± 0.05	–	–	22 ± 11
Berman et al. (2013)	–	-13.12 ± 0.06	–	–	23 ± 10
Tsuchihara et al. (2016)	–	–	–	–	22 ± 5
Present study ($n = 106$)	-188.9 ± 0.3	-13.12 ± 0.02	-24.74 ± 0.04	9.0 ± 0.18	22 ± 9

Fig. 2 Relationship between $\delta^{18}O$ and δD in each area. **a** The capital letters in the legend indicate the areas shown in Fig. 1. The equation $\delta D = 8\delta^{18}O + 12.8$ is the regression line for all data with a slope of 8. **b** Graph shows an enlarged view of the plots of the SE area
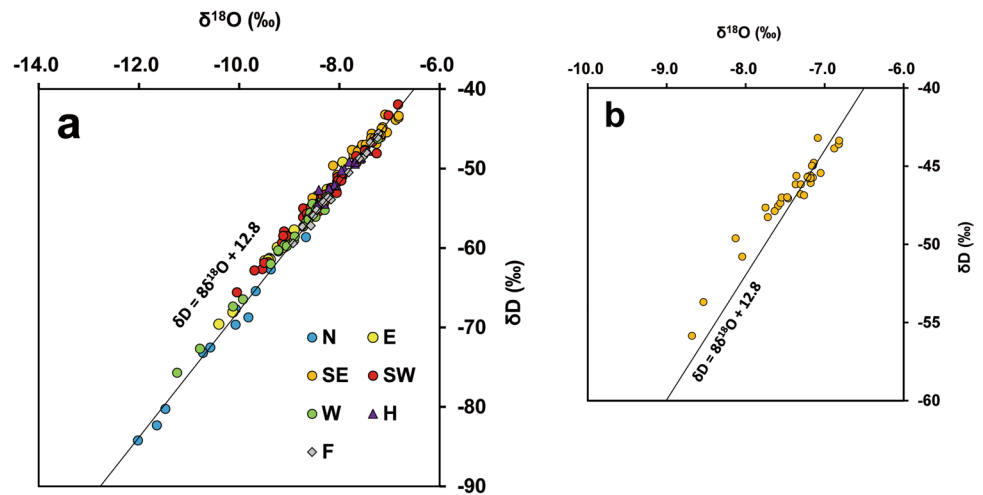
sample were conducted for enhanced precision—analytical data are presented in Table S1 of the electronic supplementary material (ESM). The average analytical errors (1σ) for δD, $\delta^{18}O$, d-excess, and ^{17}O-excess were 0.24, 0.05, and 0.3‰, and 10 per meg, respectively, indicating an ability to discuss d-excess with an accuracy <1‰.

Results

Relationship between δD, δ¹⁸O, d-excess and ¹⁷O-excess

Figure 2 and Table 3 show the relationship between $\delta^{18}O$ and δD in groundwater (spring and well), classified by area. For all data, δD ranged from −84.2 to −41.9‰, and $\delta^{18}O$ from −12.02 to −6.82‰, which is close to those of Nakai et al. (1995). Regressing all data, the relationship between $\delta^{18}O$ and δD is portrayed in Eq. (5):

$$\delta D = 7.72\delta^{18}O + 10.4 \quad \left(n = 165, R^2 = 0.986\right) \tag{5}$$

Regressing all data using a straight line with the slope of 8,

$$\delta D = 8\delta^{18}O + 12.8 \quad \left(n = 165, R^2 = 0.986\right) \tag{6}$$

Equation (6) is consistent with the results of Yasuhara et al. (2007), who found a d-excess in groundwater of 13.5. This research reveals that area N maintains relatively lighter δD (Nakai et al. 1995; Yasuhara et al. 2007) and lower d-excess compared to others. In addition, it was confirmed that the SE area groundwater held heavier δD and $\delta^{18}O$ (Yasuhara et al. 2007), and a gentle slope of $\delta^{18}O$–δD (Nakai et al. 1995).

Figure 3 shows the linear relationship between $10^3 \ln(10^{-3}\delta^{18}O + 1)$ vs. $10^3 \ln(10^{-3}\delta^{17}O + 1)$ in groundwater,
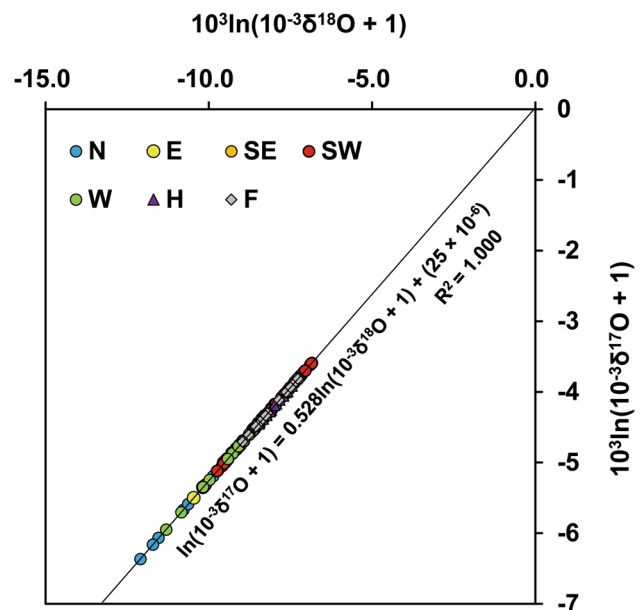
Table 3 Linear regression equations of the groundwater in each area. The SE, SW, W, and H areas maintained a gentler slope than N, E, and F. The slope of 5.9 in the SE area is close to that obtained by Nakai et al. (1995)

Area	Linear relationship	R^2
N	$\delta D = 7.9\,\delta^{18}O + 10.3$	0.987
E	$\delta D = 7.8\,\delta^{18}O + 11.3$	0.988
SE	$\delta D = 5.9\,\delta^{18}O - 2.7$	0.940
SW	$\delta D = 7.0\,\delta^{18}O + 4.5$	0.985
W	$\delta D = 7.4\,\delta^{18}O + 7.4$	0.994
H	$\delta D = 6.5\,\delta^{18}O + 0.7$	0.923
F	$\delta D = 7.8\,\delta^{18}O + 10.5$	0.993

Fig. 3 Relationship between $10^3\ln(10^{-3}\delta^{18}O + 1)$ and $10^3\ln(10^{-3}\delta^{17}O + 1)$ in each area. The regression of these plots with a slope of 0.528 yields an intercept of 25 per meg
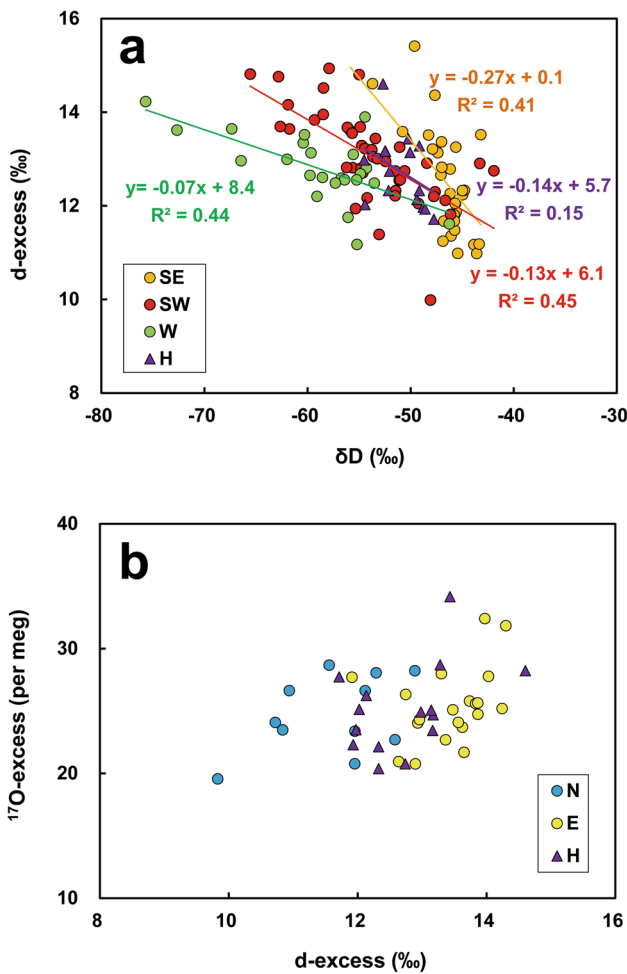
Fig. 4 a Relationship between δD and d-excess in SE, SW, W and H areas with the regression lines and the determination coefficients, R^2, of each area; **b** Relationship between d-excess and ^{17}O-excess in N, E, and H areas

$$\ln\left(10^{-3}\delta^{17}O + 1\right) = 0.528 \ \ln\left(10^{-3}\delta^{18}O + 1\right) + \left(25 \times 10^{-6}\right);$$
$$\left(n = 165, R^2 = 1.000\right) \tag{7}$$

The intercept, 25 per meg, is <33 per meg of the GMWL, and closer to the average obtained in shallow groundwater in Ibaraki, Japan (26 per meg; Tsuchihara et al. 2016).

In the present research, although δD, δ^{17}O, δ^{18}O, and the second-order parameters (d-excess and ^{17}O-excess) were analyzed and calculated, only the relationships between δD, d-excess, and ^{17}O-excess will be examined hereafter, since both δ^{17}O and δ^{18}O were well correlated with δD (Figs. 2 and 3). Regarding δD and d-excess (Fig. 4; Table 4), a negative correlation was observed in the SE, SW, W, and H areas, all of which maintained gentle slopes on the δ^{18}O–δD plot (Table 3); whereas no correlation was observed in the N, E, and F areas. From Table 4, the relationship between δD and ^{17}O-excess has $R^2 < 0.05$ for all areas except F. Because the groundwater in area F includes those mixed with the Fuji River (see section 'Division of research area'), the higher coefficient of determination is potentially erroneous, and it was concluded that δD and ^{17}O-excess do not correlate. For the relationship between d-excess and ^{17}O-excess, some R^2 values show the range 0.18–0.21 in areas N, E, and H, but the correlation was hardly observed, taking the analytical error of ^{17}O-excess into consideration ($1\sigma = 10$ per meg; Fig. 4b; Table 4).

Spatial distributions of δD, d-excess, and ^{17}O-excess

Figure 5a–c shows the spatial distributions of δD, d-excess, and ^{17}O-excess in the groundwater, and Table 5 shows the averages for each area. In Fig. 5a, δD is the heaviest in the SE area and lightest in N, tendencies that are consistent with those of Nakai et al. (1995) and Yasuhara et al. (1997, 2007). The δD in the SE area was distinct from the adjacent E, SW, and H areas. In general, at similar basin scales (10 km), the isotopic compositions of groundwater often vary spatially, but such strong divisions are rare; therefore, it was expected that the SE area has a unique background with a heavier δ value. In Fig. 5b, the d-excess spans a range of only several

regardless of the area examined. Considering the GMWL, Eq. (4), as shown by Luz and Barkan (2010), and approximating their linear relationship with a slope of 0.528, Eq. (7) is revealed:

Table 4 Regression lines and determination coefficients, R^2, between δD and d-excess, between δD and ^{17}O-excess, and between d-excess and ^{17}O-excess

Area	Between δD and d-excess		Between δD and ^{17}O-excess		Between d-excess and ^{17}O-excess	
	d-excess value	R^2	^{17}O-excess value	R^2	^{17}O-excess value	R^2
N	$-0.004\delta D + 11.4$	0.00	$0.07\delta D + 29.7$	0.03	$1.54(\text{d-excess}) + 6.9$	0.21
E	$-0.02\delta D + 12.4$	0.02	$0.03\delta D + 27.0$	0.00	$1.75(\text{d-excess}) + 1.9$	0.19
SE	$-0.27\delta D + 0.1$	0.41	$-0.06\delta D + 22.7$	0.00	$0.63(\text{d-excess}) + 17.7$	0.06
SW	$-0.13\delta D + 6.1$	0.45	$0.05\delta D + 27.0$	0.00	$-0.01(\text{d-excess}) + 24.7$	0.00
W	$-0.07\delta D + 8.4$	0.44	$0.05\delta D + 27.9$	0.01	$-0.98(\text{d-excess}) + 37.7$	0.05
H	$-0.14\delta D + 5.7$	0.15	$0.25\delta D + 37.9$	0.02	$1.97(\text{d-excess}) + 0.1$	0.18
F	$-0.02\delta D + 11.1$	0.05	$0.20\delta D + 15.4$	0.20	$-0.89(\text{d-excess}) + 36.7$	0.03

Fig. 5 Spatial distribution of: **a** δD, **b** d-excess, and **c** ¹⁷O-excess. For ▶ the high contrast, the intervals of classification in the legends are not constant (**a** and **c**)

‰, with no distinct spatial variation except in area N. The low d-excess was distributed in the N area and at low elevations along the coastline; whereas higher d-excess values were found in the E and W areas, and other locations at high elevations (except for N). Thus, both elevation and slope directions appear related to d-excess. Regarding the ¹⁷O-excess (Fig. 5c), most groundwater ranged from 23 to 27 per meg across all samples (average 25 per meg with $1\sigma \pm 3$ per meg). Almost no spatial variation was observed, but it appeared to be large at high elevations.

Altitude effects of δD, d-excess, and ¹⁷O-excess

Figure 6a–c shows the relationship between δD, d-excess, ¹⁷O-excess, and elevation in spring water. Regarding the relationship between δD and elevation (Fig. 6a), most springs were found in the region with a lapse rate of $-2.0‰ \cdot 100 \text{ m}^{-1}$, which was similar to that obtained by Yasuhara et al. (1997) and Ono et al. (2018). This altitude effect can be seen across the entire area, not within areas. Figure 6b shows the relationship between d-excess and elevation, where the observed range of the former was small, although the altitude effect was still observed in each area, except for N. Accordingly, the altitude effect of d-excess was more prominent than that of δD, and can be estimated as $0.18‰ \cdot 100 \text{ m}^{-1}$, which was within the range of $0.1–0.5‰ \cdot 100 \text{ m}^{-1}$ usually found in humid regions (see section 'Introduction'). Figure 6c shows the relationship between ¹⁷O-excess and elevation, where No. 1, located at the highest elevation in the SW area, had a large ¹⁷O-excess. Except for part of N and W areas, the elevational dependence was visible, at a lapse rate of 0.6 per meg · 100 m⁻¹, within the range of results observed on the windward side of the NW Pacific mountains in the US (0.1 and 2.3 per meg · 100 m⁻¹; Bershaw et al. 2020). For the N area (and part of W), the plotted values appear as outliers from the overall tendency, and this is true for the relationship between d-excess and elevation as well.

Discussion

Isotopic compositions of area N

The δD in the N area was significantly lighter than elsewhere (Fig. 5a), revealing a similar tendency to those found by Nakai et al. (1995) and Yasuhara et al. (2007), who proposed a conceptual model for the trajectory of water vapor masses during heavy rain. The vapor-derived precipitation
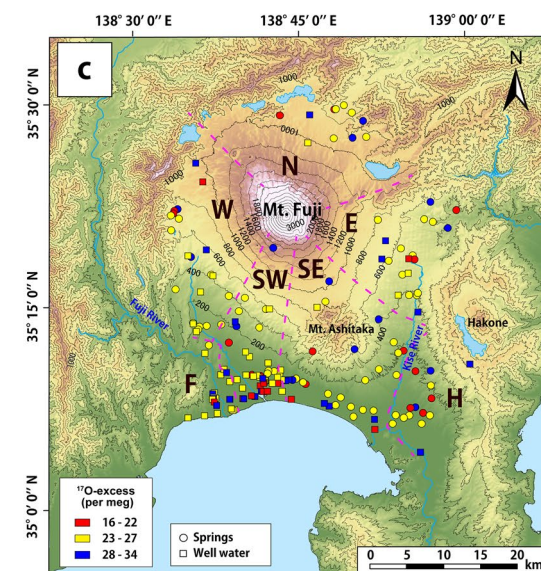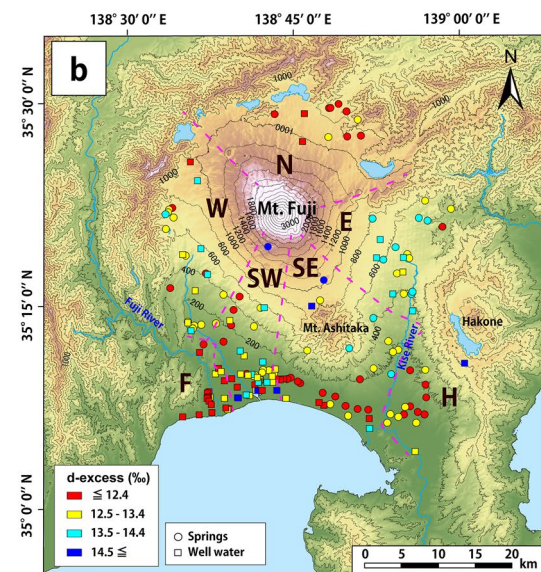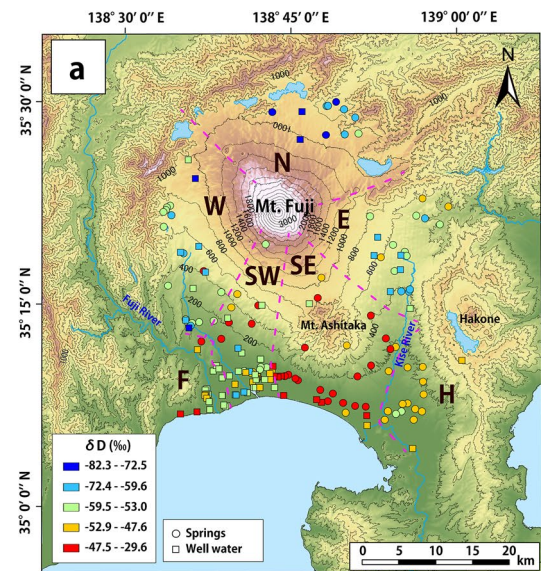
Fig. 6 Relationships between: **a** δD and spring elevation (shaded area ▶ indicates a lapse rate of −2.0‰ · 100 m⁻¹), **b** d-excess and spring elevation (lapse rate of 0.18‰ · 100 m⁻¹), and **c** ^{17}O-excess and elevation of springs (lapse rate of 0.6 per meg · 100 m⁻¹)

in the N area came mainly from area E, following heavy rains. Under the Rayleigh conditions, ^{17}O-excess should not change, depending on the degree of the rain-out progress. This vapor movement is therefore consistent with the results here, where there is nearly the same groundwater ^{17}O-excess in the E and N areas (Fig. 5c); however, Table 5 shows that the d-excess in the N area changed by >1‰ from area E, and the relationships between d-excess–elevation, and ^{17}O-excess–elevation, of spring water were outliers from the overall tendencies (Fig. 6b,c). There are several possible explanations for these phenomena: they may be related to the great change of the source of air mass in area N or the difference in the contribution of summer and winter precipitation to recharge water (Liotta et al. 2006; Dong et al. 2018). Alternatively, evaporation might affect the d-excess since the amount of precipitation at Lake Kawaguchi in the N area is small, but noticeable evaporation could not be identified from the 7.9 slope of the δ^{18}O–δD plots (Table 3). Overall, the reasons for this phenomenon remain unclear, and may possibly relate to the lower number of samples in area N compared to other areas. More research is thus needed to examine the isotopic compositions of groundwater there.

Evaporation effect and the gentle slope in δD–δ^{18}O

From Table 4 and Fig. 4, the areas with high R^2 between δD and d-excess maintained a gentle slope of the δ^{18}O–δD relationship (SE, SW, W, and H areas). Notably, the climate in the gently sloped SE area has high temperatures and low precipitation (close to Mishima City, Table 1), while the E area, which experiences high precipitation, does not show this tendency. Using Henning's formula and meteorological data (Table 1; Morimoto et al. 2013), the lifted condensation

Table 5 Average isotopic compositions in each area

	δD (‰)	δ^{18}O (‰)	d-excess(‰)	^{17}O-excess(per meg)
N	−71.4	−10.37	11.6	25
E	−58.1	−8.95	13.4	25
SE	−46.7	−7.40	12.5	26
SW	−53.7	−8.34	13.0	25
W	−59.0	−8.98	12.8	25
H	−50.9	−7.96	12.7	25
F	−52.7	−8.11	12.1	26
Total	−54.38	−8.387	12.72	25.2
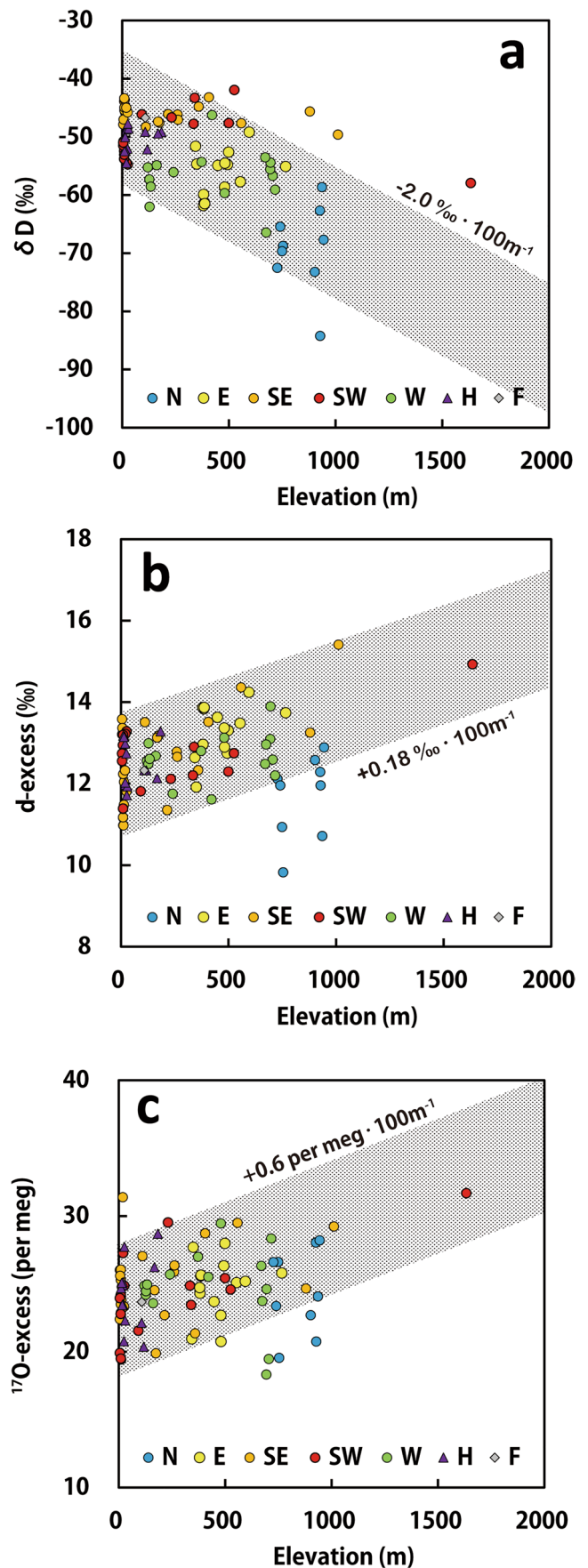
Table 6 Results of recharge elevations for five well waters (Ono et al. 2018)

Present study							Ono et al. (2018)				
No.	Elevation	Well depth	δD	δ^{18}O	d-excess	^{17}O-excess	No.	Temp.	δD	δ^{18}O	Recharge elevation
	(m)	(m)	(‰)	(‰)	(‰)	(per meg)		(°C)	(‰)	(‰)	(m)
2	579	313	−59.3	−9.14	13.8	25	W7	13.1	−60	−9.2	1,800
9	108	245	−53.4	−8.36	13.4	23	W13	14.9	−54	−8.3	1,500
10	116	246	−61.8	−9.42	13.6	23	W12	13.6	−62	−9.6	1,900
37	10	18	−53.6	−8.34	13.0	23	W28	15.7	−54	−8.2	1,500
40	6	200	−65.6	−10.05	14.8	19	W30	14.2	−66	−10.2	2,050–2,100
Analytical error			0.24	0.05	0.3	10	–	–	1	0.2	–

level around Mt. Fuji was estimated to be ~700 m asl; thus, the elevations of most springs were lower than the average cloud base in the SE area. Considering the studies conducted in humid regions (Crzu-San Julian et al. 1992; Liebminger et al. 2006; Wakiyama et al. 2013; Bershaw et al. 2020), the influence of evaporation would affect the δD, d-excess, and ^{17}O-excess in groundwater.

Calculations according to Gonfiantini (1986) were performed to quantitatively evaluate the maximum influence of evaporation on each parameter in the SE area (ESM). Assuming No. 1 (δD = −49.6‰, δ^{18}O = −8.13‰, and d-excess = 15.4‰), and No. 25 (δD = −43.6‰, δ^{18}O = −6.82‰, d-excess = 11.0‰) are given as the initial and final water states, respectively, ~6% of evaporation from the whole water body was necessary to produce a change of 4.4‰ in d-excess. For comparison, the calculation by Liebminger et al. (2006) showed that a 1% evaporation caused a change of 1‰ in d-excess under their local climatic conditions. Overall, because only a small amount of evaporation is required for the transition from the initial to final water, it seems a likely process from both qualitative and quantitative aspects. The influence of evaporation on ^{17}O-excess can be calculated in the same way. As a result, 6% of evaporation should cause only a change of 7 per meg in ^{17}O-excess, which is estimated to be the maximum change found here but less than the analytical error. The preceding calculations consistently explained why the heavy δ value and low d-excess in groundwater were distributed in the SE area, but ^{17}O-excess had a small spatial distribution (Fig. 5a–c) and revealed little correlation between d-excess and ^{17}O-excess (Fig. 4b,d; Table 4). Thus, the isotopic properties depend largely on the area. Therefore, it is necessary to analyze isotope properties within the area to determine the recharge area by using them as tracers.

Determination of recharge elevation using water temperature, δD, δ^{18}O, d-excess, and ^{17}O-excess

Ono et al. (2018) estimated the recharge elevations for five well waters (Table 6) located on a survey line in the SW area by using the recharge line, which is produced by δD in small spring water assumed to be equal to that in the recharge water shown by Yasuhara et al. (1997). In this section, the recharge elevations will be calculated in the same way, but using not only δD but also water temperature, δ^{18}O, d-excess, and ^{17}O-excess as tracers. Seven springs discharging perched water, located in the SW area (Nos. 1, 3, 4, 5, 6, 8, and 13), are assumed to represent recharge water. For groundwater temperature, the averaged data obtained by Ono et al. (2018) were used. The lapse rates were fixed as follows: the water temperature was set to −0.6 °C · 100 m^{-1}, which is the local lapse rate in the research area (Japan Meteorological Agency 2021), and δD and δ^{18}O were set to −2‰ · 100 m^{-1} and −0.24‰ · 100 m^{-1}, which were reported by Yasuhara et al. (1997) and Yasuhara et al. (2007). The lapse rates for d-excess and ^{17}O-excess were given as 0.18‰ · 100 m^{-1} and 0.6 per meg · 100 m^{-1}, respectively (from Fig. 6).

The relationship between water temperature and isotope properties was plotted within a range with a lapse rate, since they vary with respect to the elevation. Taking the analytical error into consideration, the possible recharge elevation (the range between upper and lower limits of recharge elevation) became the "RE" in Fig. 7. As a result, the range of RE for water temperature became 282 m, and 975 m for δD, 646 m for δ^{18}O, 827 m for d-excess, and 4,528 m for ^{17}O-excess. It should be noted that water temperature seems to have a small RE, but its seasonal fluctuation was not considered; nevertheless, a maximum 5 °C change was observed in these springs by Ono et al. (2018).

Figure 8 shows the upper and lower limits of the recharge elevations of the five wells in Table 6 calculated from the RE in Fig. 7. Considering the altitude effects of

Fig. 7 The relationship between measurements of each tracer and elevation of seven springs located on the slope of SW area. **d–e** The lateral bars on the d-excess and ^{17}O-excess indicate the errors of recharge elevation caused by their analysis error. Such lateral bars are not shown (**a**) as the errors are unknown. **b** and **c** Lateral bars are also not shown in due to the small size of the symbols
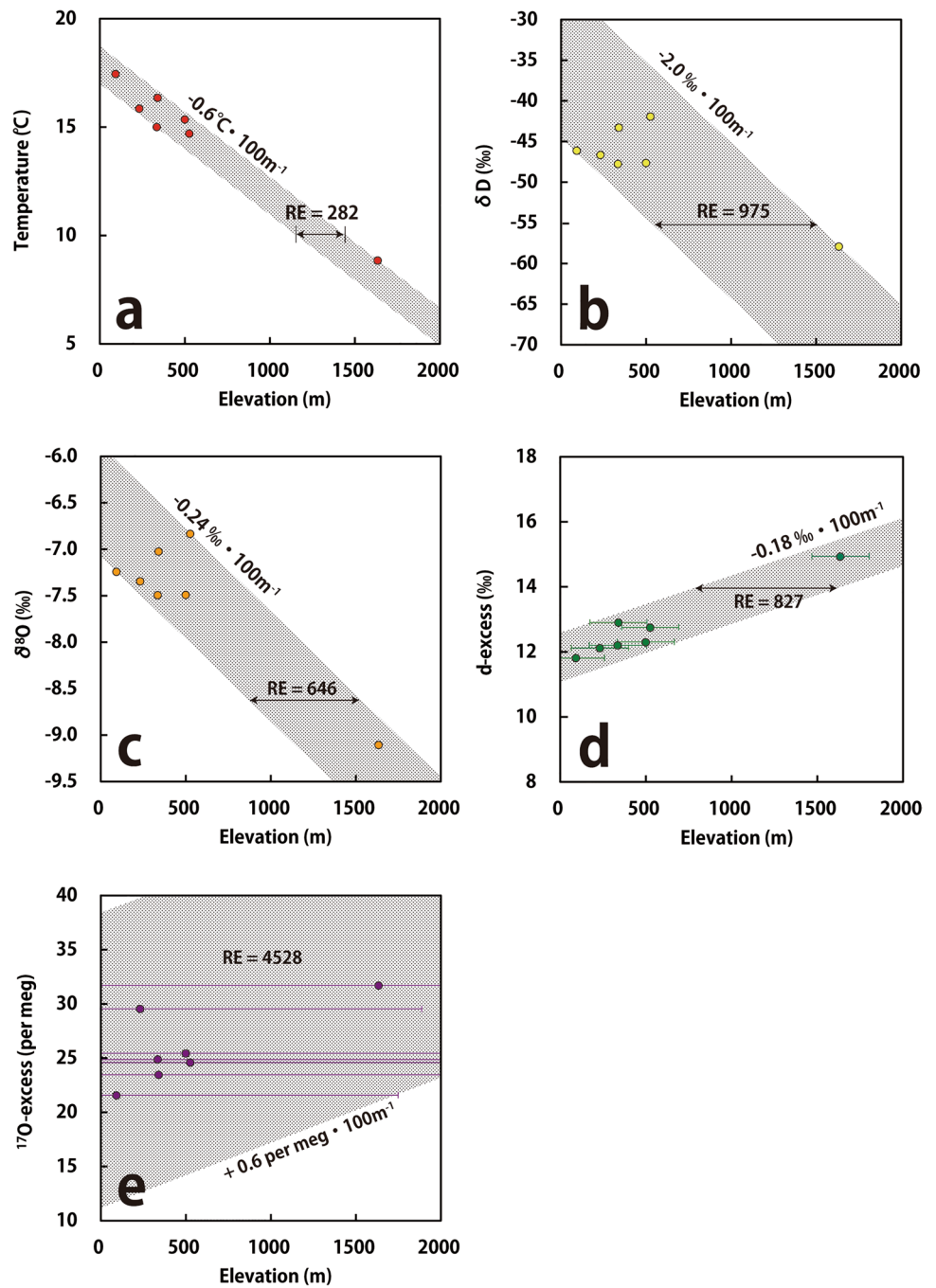
δD ($-2.0‰ \cdot 100$ m^{-1}) and $\delta^{18}O$ ($-0.24‰ \cdot 100$ m^{-1}), the effect of analytical errors for δD ($0.24‰$) and $\delta^{18}O$ ($0.05‰$) can cause 12 and 21 m of the changes in recharge elevations, respectively. Therefore, analytical errors for δD and $\delta^{18}O$ were unlikely to have caused the increase of RE. The δD and $\delta^{18}O$ do not change linearly with respect to elevation but have their own variabilities (Fig. 7); these variabilities might be due to the difference in recharge area in springs, local meteorological conditions, or degree of evaporation, which is also influenced by the permeability and vegetation on land surfaces (Gat 1971). On the other hand, d-excess seems to have small variability, but a relatively low lapse rate results in great RE (827 m) in Fig. 8. Although ^{17}O-excess seems to depend on the elevation (Fig. 6), it is difficult to apply it as a tracer, especially in a small basin because of its large analytical error ($1\sigma = 10$ per meg). It is, however, expected that it will become a useful tracer in the future by improving the analytical accuracy. In this way, the recharge elevations determined by δD, $\delta^{18}O$, and d-excess are similar (Fig. 8), which indicates the usefulness of these tracers, including d-excess.

Fig. 8 Ranges of recharge elevations for groundwater calculated using different tracers. Vertical bars show the range between upper and lower limits of recharge elevation, RE, determined by using temperature (red colored), δD (orange), δ^{18}O (light green), d-excess (green), and ^{17}O-excess (purple). The numbers in the lower part of the graph indicate the sampling point
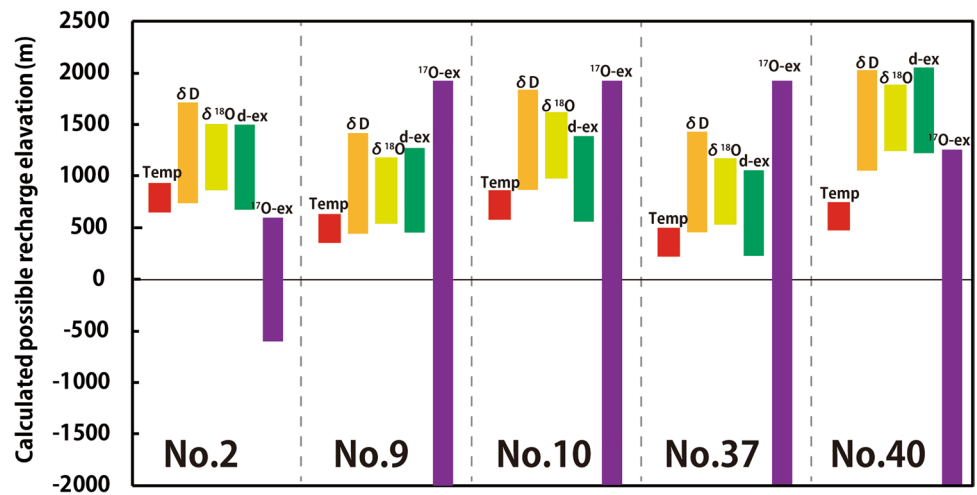
The average recharge elevation (the midpoint of upper and lower limits of recharge elevation in Fig. 8) for all well waters located in the SW area (29 points: see the ESM) were calculated using water temperature, δD, δ^{18}O, and d-excess, and compared with each other (Fig. 9). The relationship between the recharge elevations obtained by δD and δ^{18}O forms almost one straight line (Fig. 9a), and the recharge elevation is slightly higher in δD in the low elevation. On

the other hand, the plots vary, but correlations were found in δD–d-excess (Fig. 9b) and δD–water temperature (Fig. 9c). From the relationship between temperature and d-excess, a positive relationship can be seen, and the recharge elevations calculated by temperature were lower than those by d-excess (Fig. 9d). In this way, the recharge elevation calculated by the tracer increases in the order of δD > δ^{18}O > d-excess > temperature. The recharge elevation calculated from

Fig. 9 Comparison of recharge elevations of well waters calculated by using different tracers: **a** δD and δ^{18}O, **b** δD and d-excess, **c** δD and temperature, and **d** temperature and d-excess
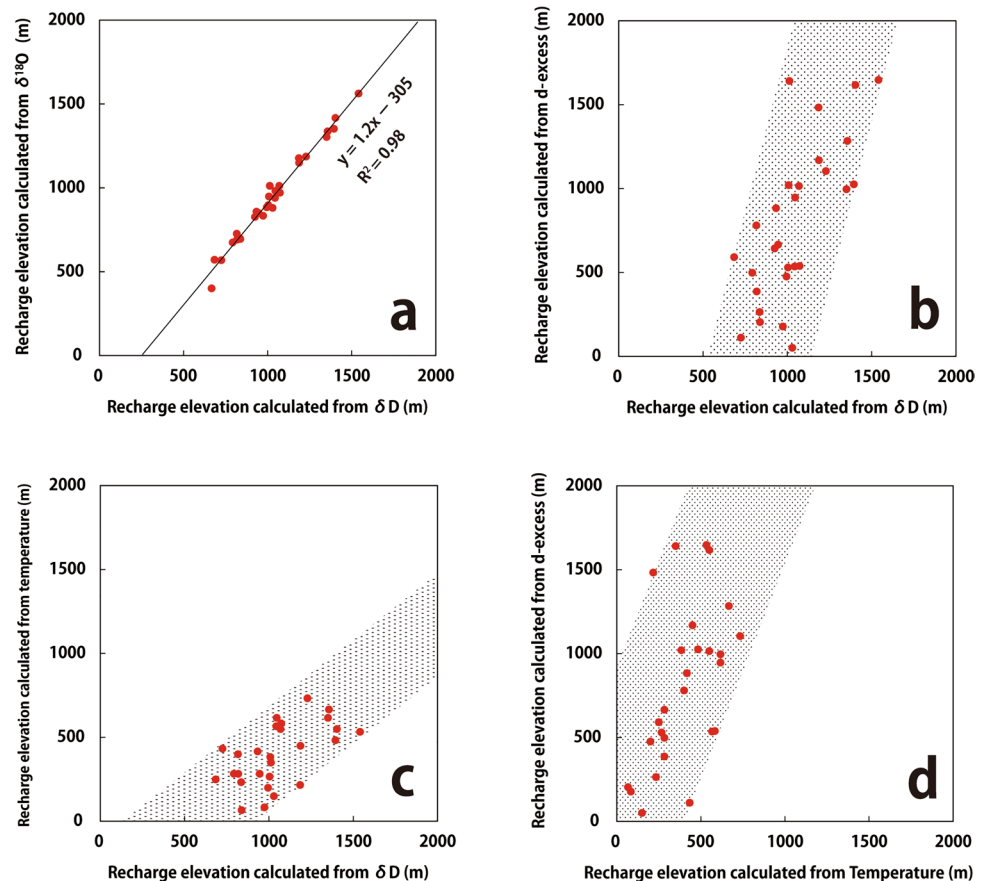
temperature could have become the lowest due to the geo-thermal gradient in the volcanic area, which raises the groundwater temperature or due to insufficient data on sea-sonal fluctuation. The reason for the difference in recharge elevations between δD, $\delta^{18}O$, and d-excess is unknown; the overlap among different tracers is an important indicator for determining the groundwater protection zones.

Conclusion

The purpose of the present study was to examine the spatial changes in stable isotopes, including d-excess and ^{17}O-excess in groundwater in a small-scale basin, and examine their usefulness to determine the recharge elevation of groundwater. For this, ~160 groundwater samples (spring and well water) were collected from slopes with different aspects at the foot of Mt. Fuji, the highest mountain in Japan. The research area maintains a humid climate with >70% RH, and 900–2,800 mm · year^{-1} of precipitation, covering an area of 40×45 km in which most springs and wells are distributed below 1,000 m (m asl).

The high-precision isotope analyses revealed the distinct characteristics of δD and d-excess in groundwater in each area. In area N, the leeward side of the wind direction was characterized by light δD and low d-excess, which was an outlier from the overall tendencies of the elevation relationship. Areas SE, SW, W, and H were characterized by a <8 slope of the $\delta^{18}O$–δD plot and a high correlation between δD and d-excess, both of which supported the evaporation effect. Although the research area is relatively small, isotope properties were different.

Accordingly, the SW area was selected for examining the usefulness of d-excess and ^{17}O-excess to determine the recharge elevations. While the d-excess had clear elevation dependency (0.18‰ · 100 m^{-1}), the ^{17}O-excess in most groundwater was ~25 per meg with a lapse rate of 0.6 per meg · 100 m^{-1}. The recharge elevation determined by d-excess was similar to those obtained from δD and $\delta^{18}O$, indicating that d-excess can be used as a tracer in a small basin. The low lapse rate compared to the analysis error ($1\sigma = 10$ per meg) of ^{17}O-excess inhibits its usefulness as a tracer. The combination of δD, $\delta^{18}O$, and d-excess can increase the reliability of the results obtained through this method. However, the reason for the difference in recharge elevations determined by different tracers could not be clarified by the present study. To enhance the isotopic tracer method, it is necessary to carry out more studies, including the application of other tracers and more intensive and long-term observation regarding groundwater.

References

Barkan E, Luz B (2007) Diffusivity fractionations of $H_2^{16}O/H_2^{17}O$ and $H_2^{16}O/H_2^{18}O$ in air and their implication for isotope hydrology. Rapid Commun Mass Spectrom 21:2999–3005. https://doi.org/10.1002/rcm.3180

Berman ESF, Levin NE, Landais AL, Li S, Owano T (2013) Measurement of $\delta^{18}O$, $\delta^{17}O$, and ^{17}O-excess in water by off-axis integrated cavity output spectroscopy and isotope ratio mass spectrometry. Anal Chem 85(21):10392–10398. https://doi.org/10.1021/ac402366t

Bershaw J, Penny SM, Garzione CN (2012) Stable isotopes of modern water across the Himalaya and eastern Tibetan plateau: implications for estimates of paleoelevation and paleoclimate. J Geophys Res Atmosphere 117(D02110). https://doi.org/10.1029/2011JD016132

Bershaw J, Hansen DD, Schauer AJ (2020) Deuterium excess and ^{17}O-excess variability in meteoric water across the Pacific Northwest, USA. Tellus Ser B Chem Phys Meteorol 72(1):1–17. https://doi.org/10.1080/16000889.2020.1773722

Clark I, Fritz P (1997) Environmental isotopes in hydrogeology. CRC, Boca Raton, FL

Craig H (1961a) Standard for reporting concentrations of deuterium and oxygen-18 in natural waters. Science 133:1833–1834. https://doi.org/10.1126/science.133.3467.1833

Craig H (1961b) Isotopic variation of meteoric waters. Science 133:1702–1703. https://doi.org/10.1126/science.133.3465.1702

Cruz-San Julian J, Araguas L, Rozanski K, Benavente J, Cardenal J, Hidalgo MC, Garcia-Lopez S, Martinez-Garrido JC, Moral F, Olias M (1992) Sources of precipitation over south-eastern Spain and groundwater recharge: an isotopic study. Tellus 44B:226–236. https://doi.org/10.3402/tellusb.v44i3.15445

Dansgaard W (1964) Stable isotopes in precipitation. Tellus 16(4):436–468. https://doi.org/10.3402/tellusa.v16i4.8993

Dong G, Weng B, Qin T, Yan D, Wang H, Gong B, Bi W, Wang J (2018) Study on the stable isotopes in surface waters of the Naqu River basin, Tibetan plateau. ScienceAsia 44:403–412. https://doi.org/10.2306/scienceasia1513-1874.2018.44.403

Ehhalt D, Knott K, Nagel NF, Vogel C (1963) Deuterium and oxygen 18 in rain water. J Geophys Res 68(13):3775–3780. https://doi.org/10.1029/JZ068i013p03775

Friedman I, Machta L, Soller R (1962) Water-vapor exchange between a water droplet and its environment. J Geophys Res 67(7):2761–2766. https://doi.org/10.1029/JZ067i007p02761

Garzione CN, Quade J, DeCelles PG, English NB (2000) Predicting paleoelevation of Tibet and the Himalaya from δ^{18}O vs. altitude gradients in meteoric water across the Nepal Himalaya. Earth Planet Sci Lett 183(1–2):215–229. https://doi.org/10.1016/S0012-821X(00)00252-1

Gat JR (1971) Comments on the stable isotope method in regional groundwater investigations. Water Res Resour 7(4):980–993. https://doi.org/10.1029/WR007i004p00980

Gat JR, Dansgaard W (1972) Stable isotope survey of the fresh water occurrences in Israel and the northern Jordan Rift Valley. J Hydrol 16(3):177–211. https://doi.org/10.1016/0022-1694(72)90052-2

Gonfiantini R (1986) Environmental isotopes in lake studies. In: Fritz P, Fontes J (eds) Handbook of environmental isotope geochemistry, 2: the terrestrial environment B. Elsevier, New York. pp 113–163

Gonfiantini R, Roche MA, Olivry JC, Fontes JC, Zuppi GM (2001) The altitude effect on the isotopic composition of tropical rains. Chem Geol 181:147–167. https://doi.org/10.1016/S0009-2541(01)00279-0

Ichiyanagi K, Tanoue M (2016) Stable isotopes in precipitation across Japan during an intensive observation period throughout 2013 (in Japanese with English abstract). J Jpn Assoc Hydrol Sci 46(2):123–138. https://doi.org/10.4145/jahs.46.123

Japan Meteorological Agency (2021) Meteorological observation data from 1976 to 2020. http://www.jma.go.jp/jma/menu/menureport.html. Accessed 3 July 2021

Jasechko S (2019) Global isotope hydrogeology: review. Rev Geophys. https://doi.org/10.1029/2018RG000627

Kendall C, McDonnell J (1998) Isotope tracers in catchment hydrology. Elsevier. https://doi.org/10.1016/B978-0-444-81546-0.50001-X

Kizawa T, Iida M, Matsuyama S, Miyawaki A (1969) Fujisan-Shizen no Nazo wo Toku- [Elucidation of the nature in Mt. Fuji]. NHK, Shibuya-ku, Japan

Landais A, Barkan E, Luz B (2008) Record of δ^{18}O and ^{17}O-excess in ice from Vostok Antarctica during the last 150,000 years. Geophys Res Lett 35(2):1–5. https://doi.org/10.1029/2007GL032096

Landais A, Risi C, Bony S, Vimeux F, Descroix L, Falourd S, Bouygues A (2010) Combined measurements of ^{17}O-excess and d-excess in African monsoon precipitation: implications for evaluating convective parameterizations. Earth Planet Sci Lett 298:104–111. https://doi.org/10.1016/j.epsl.2010.07.033

Landais A, Ekaykin A, Barkan E, Winkler R, Luz B (2012) Seasonal variations of ^{17}O-excess and d-excess in snow precipitation at Vostok station, East Antarctica. J Glaciol 58(210):725–733. https://doi.org/10.3189/2012JoG11J237

Li S, Levin NE, Chesson LA (2015) Continental scale variation in ^{17}O-excess of meteoric waters in the United States. Geochim Cosmochim Acta 164:110–126. https://doi.org/10.1016/j.gca.2015.04.047

Liebminger A, Haberhauer G, Papesch W, Heiss G (2006) Correlation of the isotopic composition in precipitation with local conditions in alpine regions. J Geophys Res Atmosphere 111:D05104. https://doi.org/10.1029/2005JD006258

Liotta M, Favara R, Valenza M (2006) Isotopic composition of the precipitations in the Central Mediterranean: origin marks and orographic precipitation effects. J Geophys Res Atmos 111:D19302. https://doi.org/10.1029/2005JD006818

Luz B, Barkan E (2010) Variations of ^{17}O/^{16}O and ^{18}O/^{16}O in meteoric waters. Geochim Cosmochim Acta 74(22):6276–6286. https://doi.org/10.1016/j.gca.2010.08.016

Machida I (2000) Spatial and temporal changes in oxygen isotopic composition of precipitation on Myakejima Island, Tokyo (in Japanese with English abstract). J Jpn Soc Hydrol Water Res 13(2):103–113. https://doi.org/10.3178/jjshwr.13.103

Machida I (2005) Oxygen and hydrogen stable isotopes of precipitation in small oceanic island. J Jpn Soc Hydrol Water Res 18(4):349–361. https://doi.org/10.3178/jjshwr.18.349

Martin P, Gröning M (2009) Reference sheet for international measurement standards VSMOW2 and SLAP2. IAEA, Vienna, Austria

Mazor E (1997) Chemical and isotopic groundwater hydrology, 2nd edn. CRC, Boca Raton, FL

Mook WG (2001) Environmental isotopes in the hydrological cycle: principle and applications, vol II. In: Atmospheric water. IHP–V, TechnicalDocuments in Hydrology, no. 39, vol 2. UNESCO, Paris

Morimoto K, Yamamoto T, Shigetani Y, Moriwaki R (2013) Effects of differences in land use on formation of clouds-field observations of cloud base level and solar radiation in Matsuyama plain (in Japanese). J JSCE Ser. B1 (Hydraul Eng) 69(4):I_1747–I_1752. https://doi.org/10.2208/jscejhe.77.1_54

Moser H, Stichler W (1974) Deuterium and oxygen-18 contents as an index of the properties of snow covers. IAHS Publ 114, pp 122–135

Nagai M, Takahashi M (2008) Geology and eruptive history of Hakone volcano, Central Japan (in Japanese with English abstract). Res Rep Kanagawa Prefect Mus Nat Hist 13:25–42

Nakai N, Kikuta N, Tsuchi R (1995) Isotopic composition of natural waters distributing around Mt. Fuji and its applications to hydrological study (in Japanese with English abstract). J Jpn Assoc Hydrol Sci 25(2):71–81

Ochiai T, Kawasaki H (1970) Behavior of groundwater flowing in lava beds (in Japanese with English abstract). Bull Agric Eng Res Stn Japan 8:67–83

Ono M, Ikawa R, Machida I, Marui A, Muranaka Y, Kamitani T, Oyama K, Ito A (2016) Water environment map, no. 9: Mt. Fuji area (in Japanese). Geological survey of Japan, Tsukuba, Japan

Ono M, Machida I, Ikawa R, Kamitani T, Oyama K, Muranaka Y, Ito A, Marui A (2018) Regional groundwater flow system in a stratovolcano adjacent to a coastal area: a case study of Mt. Fuji and Suruga Bay, Japan. Hydrogeol J 27:717–730. https://doi.org/10.1007/s10040-018-1889-9

Paar D, Mance D, Stroj A, Pavic M (2019) Northern Velebit (Croatia) karst hydrological system: results of a preliminary ^{2}H and ^{18}O stable isotope study. Geol Croat 72(3):205–213. https://doi.org/10.4154/gc.2019.15

Schoenemann SW, Schauer AJ, Steig EJ (2013) Measurement of SLAP2 and GISP δ^{17}O and proposed VSMOW–SLAP normalization for δ^{17}O and ^{17}O$_{excess}$. Rapid Commun Mass Spectrom 27(5):582–590. https://doi.org/10.1002/rcm.6486

Shikazono N, Arakawa T, Nakano T (2014) Groundwater quality, flow, and nitrogen pollution at the southern foot of Mt. Fuji (in Japanese with English abstract). J Geogr 123(3):323–342. https://doi.org/10.5026/jgeography.123.323

Scholl MA, Ingebritsen SE, Janik CJ, Kauahikaua JP (1996) Use of precipitation and ground water isotopes to interpret regional hydrology on a tropical volcanic island: Kilauea volcano area. Hawaii Water Resour Res 32(12):3525–3537. https://doi.org/10.1029/95WR02837

Siegenthaler U (1979) Stable hydrogen and oxygen isotopes in the water cycle. In: Jäger E, Hunziker JC (eds) Lectures in isotope geology. Springer, Heidelberg, Germany, pp 265–273

Steig EJ, Gkinis V, Schauer AJ, Schoenemann SW, Samek K, Hoffnagle J, Dennis KJ, Tan SM (2014) Calibrated high precision ^{17}O–excess measurement using cavity ring-down spectroscopy with laser-current-turned cavity resonance. Atmos Meas Tech 7:2421–2435. https://doi.org/10.5194/amt-7-2421-2014

Tanoue M, Ichiyanagi K, Shimada J (2013) Seasonal variation and spatial distribution of stable isotopes in precipitation over Japan (in Japanese with English abstract). J Jpn Assoc Hydrol Sci 43(3):73–91. https://doi.org/10.4145/jahs.43.73

Tsuchihara T, Yoshimoto S, Shirahata K, Ishida S (2016) ^{17}O–excess and stable isotope compositions of rainwater, surface water and groundwater in paddy areas in Ibaraki, Japan (in Japanese). IDRE J 302(84–2):I_185–I_194

Uemura R, Barkan E, Abe O, Luz B (2010) Triple isotope composition of oxygen in atmospheric water vapor. Geophys Res Lett 37:L04402. https://doi.org/10.1029/2009GL041960

Ueno T, Ishihara K, Yamauchi F, Saito M, Tanaka Y, Hirata K (1998) Examination on present conditions of water circulation in Kisegawa River/Obagawa River basin and preservation of Kakitagawa/Mishima peripheral welling waters: for preservation of groundwater in Fuji, Hakone and Ashitakayama area covered with volcanic sedimentary soil (in Japanese). J Ground Water Tech 40(6):1–13

Wakiyama Y, Makino Y, Yamanaka T, Suzuki K (2013) Spatiotemporal variations in deuterium excess of precipitation over the Japanese Alps region. J Geogr 122(4):666–681. https://doi.org/10.5026/jgeography.122.666

Wise S, Watters R (2012) Report of investigation reference material 8536 GISP Greenland Ice Sheet precipitation. IAEA, Vienna, Austria

Yamanaka T (2020) Tracing the hydrological cycle using environmental isotopes (in Japanese). Kyoritu Shuppan, Tokyo

Yamanaka T, Suzuki K, Wakiyama Y, Kishi K, Kakino Y, Maruyama K, Kano M, Ma W, Masaki D, Sugiyama M, Yamakawa Y, Yoshitake S (2016) Isotope mapping on mountainous regions: current state and way forward (in Japanese with English abstract). J Jpn Assoc Hydrol Sci 46(2):73–86. https://doi.org/10.4145/jahs.46.73

Yasuhara M, Marui A, Kazahaya K (1997) Stable isotopic composition of groundwater from Mt. Yatsugatake and Mt. Fuji, Japan. Proc. of the Rabat Symp., IAHS Publ. 244, IAHS, Wallingford, UK, pp 335–344

Yasuhara M, Kazahaya K, Marui A (2007) An isotopic study on where, when, and how groundwater is recharged in Fuji volcano, central Japan (in Japanese with English abstract). In: Aramaki S, Fujii T, Nakada S, Miyaji N (eds) Fuji volcano. Yamanashi Institute of Environmental Sciences, Kofu, Japan, pp 389–405

Yui M, Fujii T (1989) Geology of Ashitaka volcano, Central Japan (in Japanese with English abstract). Bull Earthquake Res Inst 64(2):347–389

Yurtsever Y, Gat JR (1981) Atmospheric water. In: Stable isotope hydrology, deuterium and oxygen–18 in the water cycle. Technical report series 210, IAEA, Vienna, pp 103–142